Electronic Supplementary Material (ESI) for Journal of Materials Chemistry A
This journal is © The Royal Society of Chemistry 2019

Electronic Supporting Information

Highly Stretchable, Ultra-tough, Remarkably Tolerant, and Robust Self-Healing Glycerol-Hydrogel for Dual-Responsive Soft Actuator

Meiling Guo, [a] Yuanpeng Wu,*[a,b] Shishan Xue, [a] Yuanmeng Xia, [a] Xi Yang, [a] Yuris Dzenis, [c] Zhenyu Li,*[a] Weiwei Lei, [d] Andrew T. Smith [e] and Luyi Sun*[e]

a. School of Material Science and Engineering, Southwest Petroleum University, Chengdu 610500, Sichuan, China, E-mail: ypwu@swpu.edu.cn

b. State Key Laboratory of Oil and Gas Reservoir Geology and Exploitation, Southwest Petroleum University, Chengdu 610500, Sichuan, China, E-mail: ypwu@swpu.edu.cn

c. Department of Engineering Mechanics, Nebraska Center for Materials and Nanoscience, University of Nebraska-Lincoln, Lincoln, NE 68588-0526, USA

d. Institute for Frontier Materials, Deakin University, Locked Bag 2000, Geelong, Victoria 3220, Australia

e. Polymer Program, Institute of Materials Science and Department of Chemical and Biomolecular Engineering, University of Connecticut, Storrs, CT 06269, USA, E-mail: luyi.sun@uconn.edu

This file includes:

1. Supplementary Experimental Section

2. Supplementary Table S1-S5

3. Supplementary Figure S1-S12

4. Supplementary Video S1-S3

1. Supplementary Experimental Section

Materials: Functionalize boron nitride nanosheets (f-BNNSs) was prepared and characterized according to our previous reports.[1,2] Acrylamide (AM, 99%), maleic anhydride (MAH, 99%), tetramethyl ethylenediamine (TEMED, 99%) were purchased from Sigma-Aldrich. Potassium persulfate (KPS; 99.0%), glycerol (99.0%) were purchased from Aladdin Industrial Corporation. All these chemicals were analytical grade used as received without further purification.

Preparation of P(AM-co-MAH)/f-BNNS Glycerol-Hydrogels: The f-BNNSs were first dispersed in deionized water and sonicated for 30 min to fabricate the homogeneously and steadily distributed f-BNNS dispersions. Subsequently, AM and MAH were dispersed in the suspension by vigorous stirring in an ice-water bath for 30 min. After that, KPS and TEMED were added under stirring and N_2 was bubbled into the solution for 10 min to remove oxygen. The solution was held at 40 °C in a water bath for 8 h to fabricate the P(AM-*co*-MAH)/f-BNNS hydrogel. The specific quantity of each component is listed in Table S1 and Table S2. Finally, the P(AM-*co*-MAH)/f-BNNS hydrogel was cut into strips of 3 mm wide, 2 mm thick and 30 mm length, and then immersed in 66.7 wt.% glycerol-water solution to fabricate the P(AM-*co*-MAH)/f-BNNS glycerol-hydrogel.

Preparation of Hydrogel and Glycerol-Hydrogel Hybrids: The f-BNNS monomer solution was prepared with the above method. And the as-prepared solution is transferred to the corresponding mold, including a homemade mold consisting of two glass plates (2 mm) and one silica plate (1 mm), syringes with diameter of 1 cm. Then, the mold was left at 40 °C for 8 h to fabricate the P(AM-*co*-MAH)/f-BNNS hydrogel layer. Similarly, the P(AM-*co*-MAH)/f-BNNS glycerol-hydrogel layer was obtained by soaking the P(AM-*co*-MAH)/f-BNNS hydrogel in 66.7 wt.% glycerol-water solution for 20 min and then the glycerol-hydrogel was placed in a 60 °C/40% relative humidity environment for 24 h. After that, the hydrogel layer and glycerol-hydrogel layer were bonded together through hydrogen bonding. For ease of distinguishing the hydrogel layer, the layer was dyed with Rhodamine B (red). In addition, flower and cross-type silica plates were used to prepare flower structure hybrids and grippers.

Characterizations: Transmission electron microscopy (TEM) data were collected with a Hitachi H-600 operated at 200 kV. Fourier transform infrared (FTIR) spectroscopy of the samples were recorded using Thermo Scientific Nicolet 6700 spectrometer in attenuated total reflection (ATR) mode with a resolution of 4 cm^{-1} within the range 400-4000 cm^{-1}. The P(AM-*co*-MAH)/f-BNNS hydrogel and P(AM-*co*-MAH)/f-BNNS glycerol-hydrogel were investigated for their freezing temperature using a differential scanning calorimeter (DSC, TA Instruments Q20). The cooling cycle was performed from 10 °C to -80 °C at a rate of 5 °C/min. The rheological measurements of the hydrogels were performed on a HAAKE rheometer (MARS III). The storage modulus (G′) and loss modulus (G”) of the hydrogels were determined under oscillation frequency mode. The shear rate was set from 0.1 to 100 rad/s, with a constant strain of 1%.

Dehydration Resistant: To demonstrate the long-term stability and anti-dehydration, the samples (P(AM-*co*-MAH)/f-BNNS hydrogels and P(AM-*co*-MAH)/f-BNNS glycerol-hydrogels were placed at different temperature (-45 °C , 25 °C and 60 °C and) for 3 days. The ambient humidity is 90% at -45°C, 50% at 25°C and 40% at 60°C and the weight change of the samples during dehydration tests was recorded at pre-determined intervals. The anti-dehydration was characterized by the ratio of the initial weight of the hydrogels (W_0) to the weight of hydrogel at different time (W_t).

Liquid content: The liquid content before 3-day exposure (W_l) was obtained through the equation:

$$W_l = (m_t - m_0 + m_0 \times W_0)/m_t \times 100\% \qquad (1)$$

where m_t, m_0, and W_0 were weight of hydrogels after soaking in glycerol-water solution, initial weight of hydrogels and initial water content of hydrogels, respectively. W_0 is the ratio of the water content to the total weight of the hydrogels and is a fixed value of 76%.

The equilibrium mass percentage (W_q) was calculated by the formula:

$$W_q = M_q/m_t \times 100\% \qquad (2)$$

M_q was the weight of hydrogel at equilibrium exposure time. The residual liquid content after 3-day exposure (W_r) was obtained through the equation:

$$W_r = [M_q - m_0(1-W_0)]/M_q = [1-(1-W_l)/W_q] \times 100\% \qquad (3)$$

Volume variation: The volume variation after 24h exposure (V_S) under different temperatures was obtained through the equation:

$$V_s = (V_1 - V_0)/V_0 \times 100\% = (d_1^2 h_1 - d_0^2 h_0)/d_0^2 h_0 \times 100\% \qquad (4)$$

where V_0 and V_1 were the volume of the hydrogels before and after 24h exposure under different temperatures, where d_1 and h_1 were the diameter and thickness of the hydrogels after 24h exposure under different temperatures, where d_0 and h_0 were the diameter and thickness of the hydrogels before 24h exposure under different temperatures, d_0 and h_0 were fixed value of 13mm and 2mm.

Mechanical testing: Prior to the mechanical testing, three samples were stored at a humidity of 90% at -45°C, 50% at 25°C and 40% at 60°C, for one day. Then, the sample was transferred to the sealed bag immediately. And after about 5 minutes, the sample was restored to 25°C and the test was started. The tensile test was carried out using electrical universal material testing machine (Instron 2360) with a 200 N load cell under a loading rate of 50 mm/min at 25°C and humidity of approximately 50%. As-prepared hydrogel samples with the thickness of 2 mm were cut into stripes (30 mm in length, 3 mm in width). The gauge length between the clamps was 10 mm. The tensile stress (σ) representing strength was obtained through the equation:

$$\sigma = F/ (a \times b) \qquad (5)$$

where F, a, and b were force of loading and width and thickness of hydrogels, respectively. The tensile strain (ε) representing stretchability was calculated by the formula:

$$\varepsilon = (l - l_0)/l_0 \times 100\% \qquad (6)$$

where l and l_0 the were break length and the original length, respectively. The young' modulus was calculated from the slope over 0–10% strain of the stress–strain curve. The fracture toughness (U) of the samples was calculated by integrating the area under the stress-strain curve:

$$U = \int \sigma \, d\varepsilon. \qquad (7)$$

Self-Healing: The rod-shaped samples (30 mm length and 5 mm diameter) were cut into halves, incisions were highlighted by the stain of rhodamine B and the two separate halves were brought into contact immediately without applied stress in air. Then the samples were healed at -45 °C with 90% humidity, 25 °C with 50% humidity and 60 °C with 40%, respectively. After self-healing in different environments, the samples were stretched to evaluated self-healing properties. The glycerol-hydrogel was stored for three months in an environment with varying temperatures and humidities, then the self-healing capability of the sample was tested. The samples with a thickness of 2 mm were cut into stripes (30 mm in length, 3 mm in width) for tensile test.

2. Supplementary Tables S1-S5

Table S1. Composition of the glycerol-hydrogels without f-BNNSs.

MAH/AM weight ratio	MAH (g)	AM (g)	H_2O (ml)	f-BNNS/ (MAH+AM) (wt.%)	KPS (mg)	TMEDA (μL)	glycerol-water post-treatment time (min)
1:1	0.3	0.3	4	0	6	4	40
1:2	0.2	0.4	4	0	6	4	40
1:3	0.15	0.45	4	0	6	4	40
1:5	0.1	0.5	4	0	6	4	40

Table S2. Glycerol-hydrogels were prepared under varied f-BNNS contents.

MAH/AM weight ratio	MAH (g)	AM (g)	H_2O (ml)	f-BNNS/ (MAH+AM) (wt.%)	KPS (mg)	TMEDA (μL)	glycerol-water post-treatment time (min)
1:5	0.1	0.5	4	0	6	4	40
1:5	0.1	0.5	4	0.1	6	4	40
1:5	0.1	0.5	4	0.2	6	4	40
1:5	0.1	0.5	4	0.3	6	4	40

Table S3. Glycerol-hydrogels were prepared under varied glycerol-water post-treatment time.

MAH/AM weight ratio	MAH (g)	AM (g)	H_2O (ml)	f-BNNS/ (MAH+AM) (wt.%)	KPS (mg)	TMEDA (μL)	glycerol-water post-treatment time (min)
1:5	0.1	0.5	4	0.2	6	4	0
1:5	0.1	0.5	4	0.2	6	4	20
1:5	0.1	0.5	4	0.2	6	4	40
1:5	0.1	0.5	4	0.2	6	4	60
1:5	0.1	0.5	4	0.2	6	4	120
1:5	0.1	0.5	4	0.2	6	4	180

Table S4. Liquid content of the glycerol-hydrogels before and after 3 days of exposure to different environments .

glycerol-water post-treatment time (min)	W_l/ wt %	-45℃		25℃		60℃	
		W_q/ wt %	W_r/ wt %	W_q/ wt %	W_r/ wt %	W_q/ wt %	W_r/ wt %
0	76.0	100	76.0	27.7	13.4	24.0	0
20	68.7	100	68.7	67.6	53.7	56.6	45.4
40	69.1	100	69.1	73.1	57.7	60.4	48.8
60	70.4	100	70.4	84.2	64.8	65.9	55.1
120	71.1	100	71.1	85.1	66.0	68.0	57.5
180	72.3	100	72.3	85.6	67.6	69.1	59.9

W_l: the liquid content before 3-day exposure; W_q: the equilibrium mass percentage; W_r: the residual liquid content after 3-day exposure.

Table S5. The volume variation of hydrogels after 24h of exposure to different environments.

the temperatures of environments	the P(AM-*co*-MAH)/f-BNNS hydrogel			the P(AM-*co*-MAH)/f-BNNS glycerol-hydrogels		
	d_1/ mm	h_1/ mm	V_S/%	d_1/ mm	h_1/ mm	V_S/ %
-45	13	2.0	0	13	2.0	0
25	8	1.7	-67.8	12	1.9	-19.1
60	7	1.5	-78.3	11	1.9	-31.9

d_1: the diameter of the hydrogels after 24h exposure; h_1 the thickness of the hydrogels after 24h exposure; V_S: The volume variation after 24h of exposure.

3. Supplementary Figures S1-S12

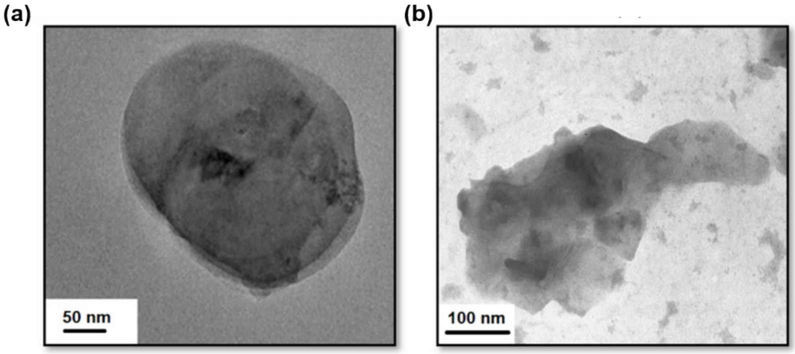

Fig. S1 TEM image of BNNSs (a), TEM image of f-BNNSs (b).

Supplementary explanation: Typical TEM images before and after poly (2-acrylamido-2-methyl-propanesulfonate) (PAMPS) grafting have been provided in Fig S2. Before grafting, BNNSs have flat surface and the lateral dimensions of BNNSs are 200 nanometers. After grafting, dark clouds, namely, PAMPS brushes can be clearly detected.[1]

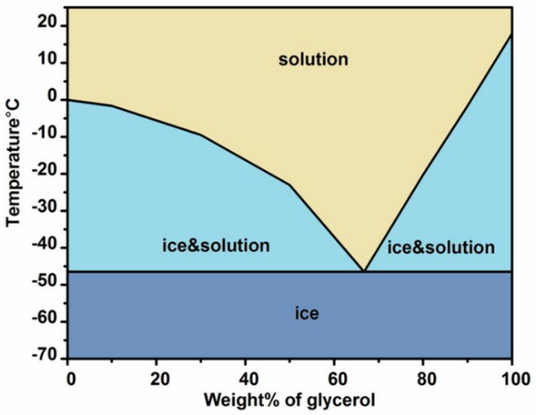

Fig. S2 Phase diagram of glycerol-water mixed solution.

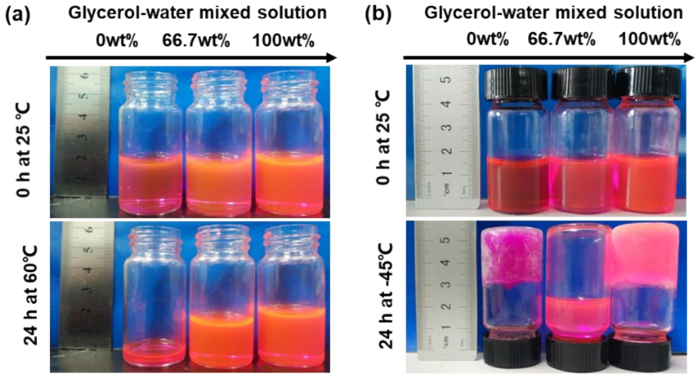

Fig. S3 Photos on water retention of different glycerol-water solutions keep at 60 °C for 24h (a); The anti-freezing performance of the glycerol-water solutions keep at -45 °C for 24h (b).

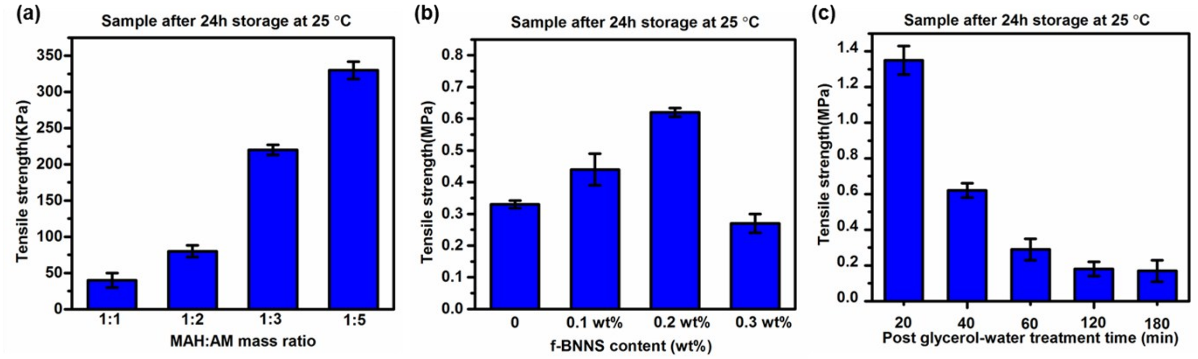

Fig. S4 Effect of mass ratio of MAH:AM (a), f-BNNS content (b) and glycerol-water post-treatment time (c) on the tensile strength of P(AM-*co*-MAH)/f-BNNS glycerol-hydrogels.

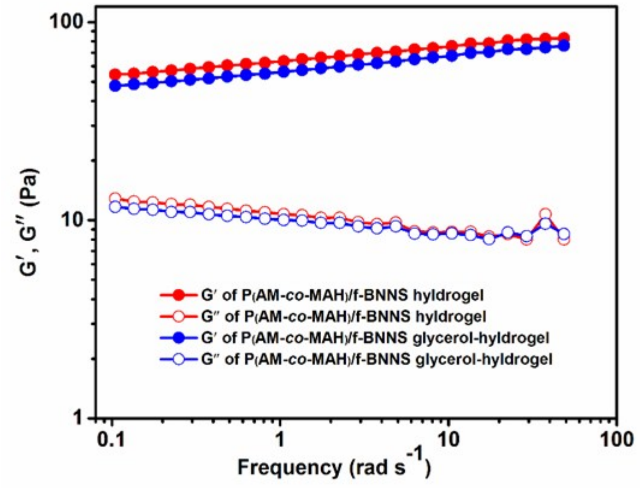

Fig. S5 Rheology profiles of P(AM-*co*-MAH)/f-BNNS hydrogel and P(AM-*co*-MAH)/f-BNNS glycerol-hydrogel.

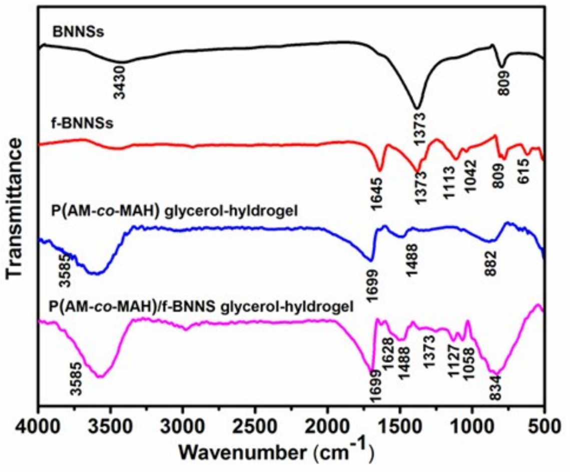

Fig. S6 FTIR spectra of BNNSs, f-BNNSs, and the glycerol-hydrogels.

Supplementary explanation: The spectrum of BNNS displays the characteristic peaks at 1373 and 809 cm^{-1}, corresponding to B-N in plane stretching and B-N-B out of plane vibrations, respectively.[3] The presence of PAMPS brushes on the surface of BNNS are confirmed by the characteristic peaks at 1645, 1113, and 1042 cm^{-1}, which correspond to -CONH- group, asymmetric and symmetric stretching vibration absorption band of sulfonic acid group, respectively.[1] The absorptions of P(AM-*co*-MAH) glycerol-hydrogel at 3585, 1699, 1488, and 882 cm^{-1} are attributed to -OH, -CONH$_2$, COO and C-O-C of glycerol and P(AM-*co*-MAH) chains, respectively.[4] Furthermore, the P(AM-*co*-MAH)/f-BNNS glycerol-hydrogel also displays the characteristic peaks of -OH, -CONH$_2$, COO and B-N at 3585, 1699, 1488, and 1373 cm^{-1}, respectively.[5,6] However, the peaks of -CONH- and the asymmetric and symmetric stretching vibration absorption band of -SO$_3$ groups are shifted to 1628, 1127 , and 1058 cm^{-1}, respectively, which indicates a strong interaction between f-BNNSs, glycerol, and P(AM-*co*-MAH) chains in hydrogel.[7]

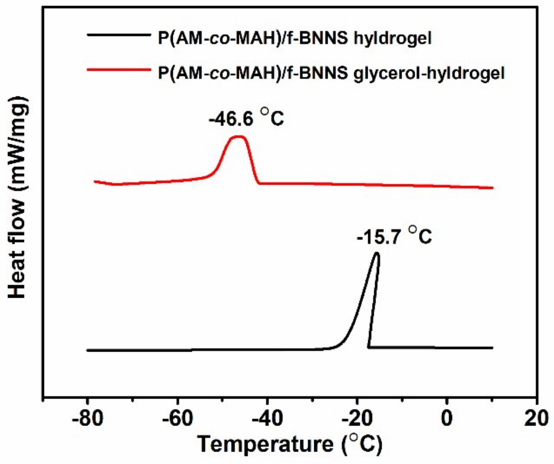

Fig. S7 DSC thermograms of the P(AM-*co*-MAH)/f-BNNS hydrogel and glycerol-hydrogels.

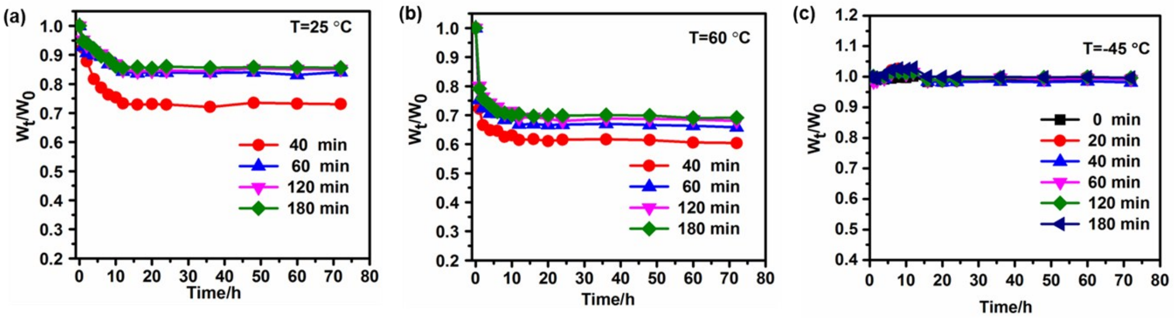

Fig. S8 Effect of immersion time on the weight change of the glycerol-hydrogels at different temperature.

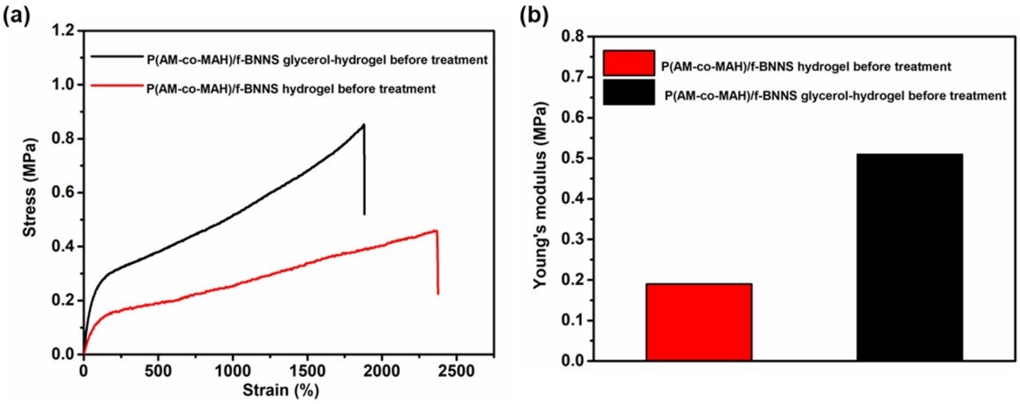

Fig. S9 Stress-strain curves (a), and Young's modulus (b) of the P(AM-*co*-MAH)/f-BNNS hydrogel and the P(AM-*co*-MAH)/f-BNNS glycerol-hydrogel before treatment.

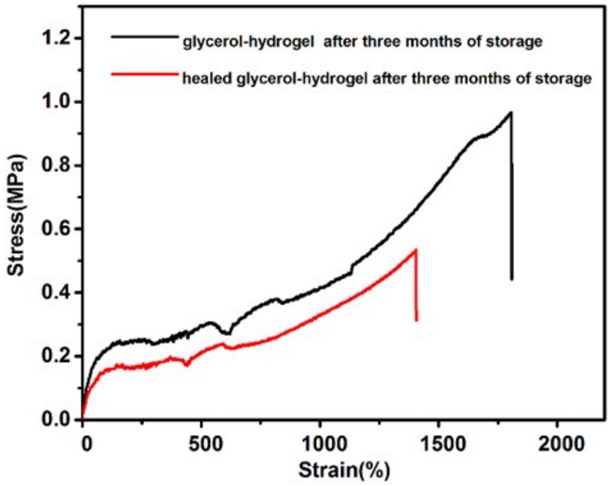

Fig. S10 Stress-strain curves of P(AM-*co*-MAH)/f-BNNS glycerol-hydrogel and the healed glycerol-hydrogel after three months of storage.

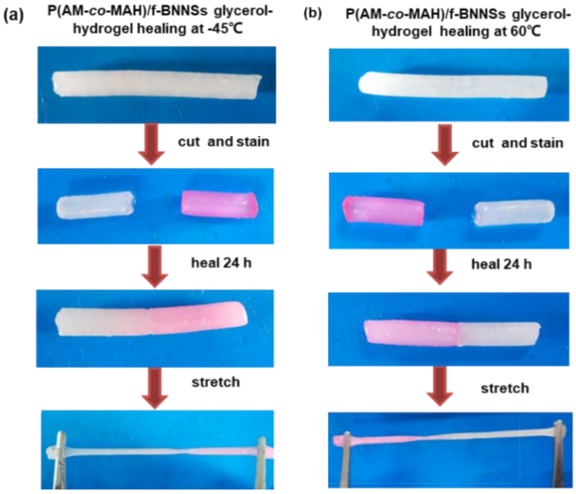

Fig. S11 Self-healing performance of the P(AM-*co*-MAH)/f-BNNS glycerol-hydrogel at -45°C (a) and 60 °C (b).

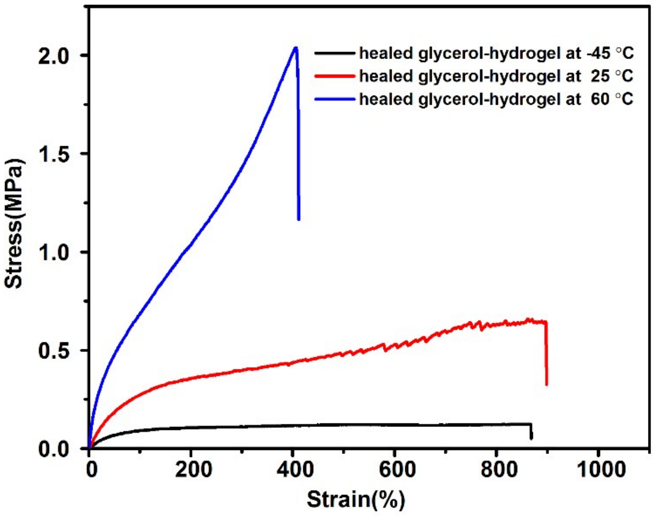

Fig. S12 Stress-strain curves of the P(AM-*co*-MAH)/f-BNNS glycerol-hydrogel healed at different temperature.

4. Supplementary Videos S1-S3

Video S1. Shape change of flower-shaped actuator under a 80 °C/30% RH environment. The movie is played at 3 X normal speed.

Video S2. Shape change of four-armed gripper under a 80 °C/30% RH environment. The movie is played at 8 X normal speed.

Video S3. Shape change of actuator under a 30 °C/30% RH environment. The movie is played at 4 X normal speed.

References

1 Y. Wu, M. Guo, G. Liu, S. Xue, Y. Xia, D. Liu and W. Lei, *Mater. Res. Express*, 2018, **5**, 045026.

2 Y. Wu, Y. Xue, S. Qin, D. Liu, X. Wang, X. Hu, J. Li, X. Wang, Y. Bando, D. Golberg, Y. Chen, Y. Gogotsi and W. Lei, *ACS Appl. Mater. Interfaces*, 2017, **9**, 43163–43170.

3 W. Lei, V. N. Mochalin, D. Liu, S. Qin, Y. Gogotsi and Y. Chen, *Nat. Commun.*, 2015, **6**, 8849.

4 C. Pan, L. Liu, Q. Chen, Q. Zhang and G. Guo, *ACS Appl. Mater. Interfaces*, 2017, **9**, 38052–38061.

5 X. Hu, J. Liu, Q. He, Y. Meng, L. Cao, Y. P. Sun, J. Chen and F. Lu, *Nanoscale*, 2016, **8**, 4260–4266.

6 R. Guo, Q. Su, J. Zhang, A. Dong, C. Lin and J. Zhang, *Biomacromolecules*, 2017, **18**, 1356–1364.

7 R. Tamate, K. Hashimoto, T. Horii, M. Hirasawa, X. Li, M. Shibayama and M. Watanabe, *Adv. Mater.*, 2018, **30**, 1802792.